

CONF-890752--3  
UCRL-100203  
PREPRINT

Received by OSTI

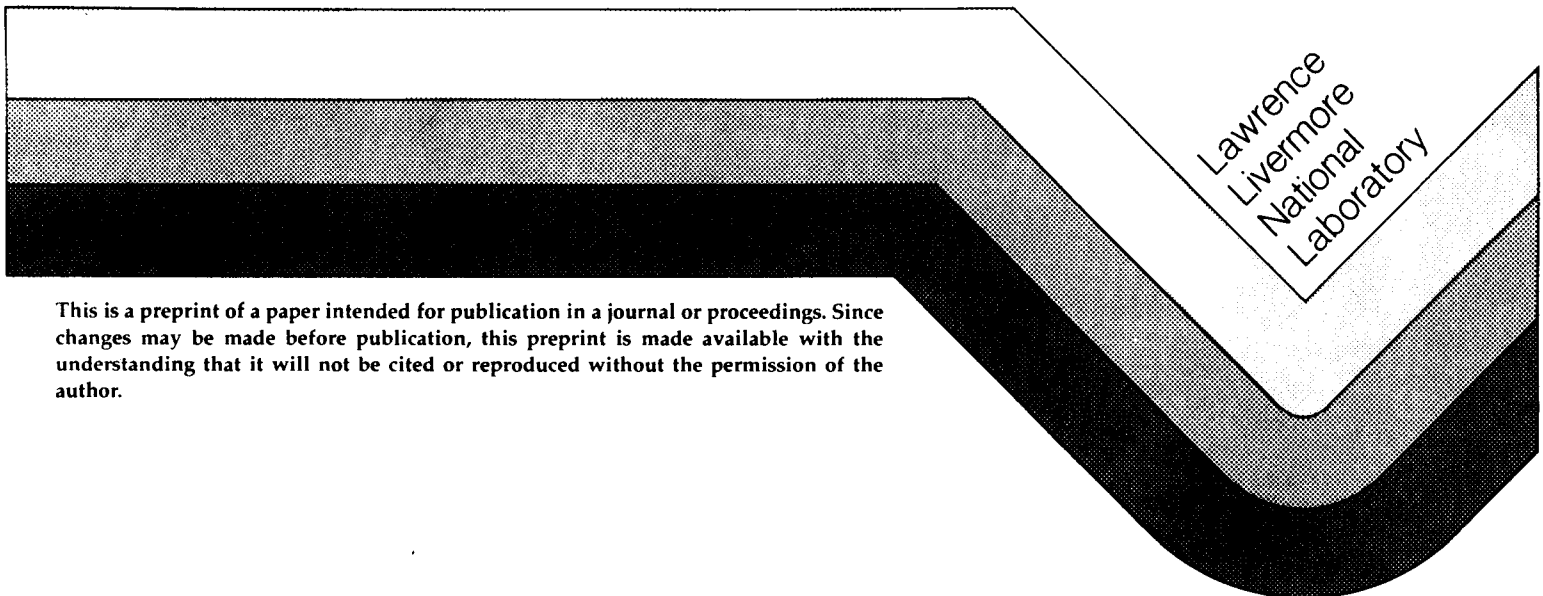
MAY 30 1989

**NUMERICAL STUDIES  
OF SHOCK WAVE STRUCTURE SENSITIVITY  
TO INTERACTIONS WITH TURBULENT FIELDS**

Alfred C. Buckingham

This is a preprint of a paper to be presented and published as part of the Proceedings of the 6th International Conference on Numerical Methods in Laminar and Turbulent Flow. Swansea, UNITED KINGDOM, July 11-15, 1989

April 1989



This is a preprint of a paper intended for publication in a journal or proceedings. Since changes may be made before publication, this preprint is made available with the understanding that it will not be cited or reproduced without the permission of the author.

DISTRIBUTION OF THIS DOCUMENT IS UNLIMITED

## **DISCLAIMER**

**This report was prepared as an account of work sponsored by an agency of the United States Government. Neither the United States Government nor any agency thereof, nor any of their employees, makes any warranty, express or implied, or assumes any legal liability or responsibility for the accuracy, completeness, or usefulness of any information, apparatus, product, or process disclosed, or represents that its use would not infringe privately owned rights. Reference herein to any specific commercial product, process, or service by trade name, trademark, manufacturer, or otherwise does not necessarily constitute or imply its endorsement, recommendation, or favoring by the United States Government or any agency thereof. The views and opinions of authors expressed herein do not necessarily state or reflect those of the United States Government or any agency thereof.**

---

## **DISCLAIMER**

**Portions of this document may be illegible in electronic image products. Images are produced from the best available original document.**

## NUMERICAL STUDIES OF SHOCK WAVE STRUCTURE SENSITIVITY TO INTERACTIONS WITH TURBULENT FIELDS

Alfred C. Buckingham

Center for Compressible Turbulence, Lawrence Livermore National Laboratory,  
University of California, Livermore, California 94550, USA<sup>(I)</sup>

### SUMMARY

This paper concerns the observed random changes to velocity, density, temperature, and pressure distributions induced in shock waves when weak shocks interact with relatively intense turbulence. Here numerical procedures are applied in order to examine this interaction process and to simulate its influence on turbulence. This interaction may be used as a diagnostic for ascertaining the distribution of interaction energy between competitive acoustic, entropy and vortical modes. Numerical procedures used here are supplements to physical experiments for tracking the dynamical mechanisms which may control the evolution of shock-turbulence interaction. The results are intended to provide assistance in the development and refinement of compressible turbulent closure models. They are obtained from use of a mixed Eulerian-Lagrangian semicontinuous rezoning finite difference method, a hybrid Euler/Lagrange pseudospectral method, and a Monte-Carlo random-choice procedure. The latter effectively magnifies the shock front region through use of finite range shock-transition integrals generating simulated interactive transition profiles.

### 1. INTRODUCTION

These numerical simulations and analyses make use of the computer as a digital tool to expand shockwave dimensions that are too small or time intervals too brief to permit adequate experimental access. The procedure models the evolution of structure (velocity, temperature, density profiles) within a spatially and temporally distorted shock front. Shock distortions develop as the shock front advances through and interacts with upstream turbulence.

(I) Work performed under the auspices of the U.S. Department of Energy by Lawrence Livermore National Laboratory under Contract No. W-7405-ENG-48.

This work is a continuation of previous analyses on the interaction of shock waves with turbulence. Conceptually, shockwave interactions couple directed shockwave translational energy into turbulence kinetic energy during shock transition. The intensity of the turbulence is amplified and its spectra altered. The changes to the turbulence characteristics apparently are most pronounced when relatively low Mach Number shockwaves encounter strong turbulence. However, some evidence and considerable theoretical speculation suggests that significant shock enhancement of turbulence may be evident at higher Mach Numbers.

Zang, Hussaini, and Bushnell [1] examined the shock turbulence amplification process using detailed numerical Euler equation simulations. Their work provided a foundation for check, confirmation and, indeed, some algebraic corrections to an existing linearized analytical prediction. The linearized predictions were developed from small perturbation theory applied as quasi-stationary boundary conditions to an undistorted, plane shock surface[2].

Subsequently, Navier-Stokes numerical simulations were developed to help define the influence of viscosity on the spatial and temporal persistence of the turbulence amplification [3].

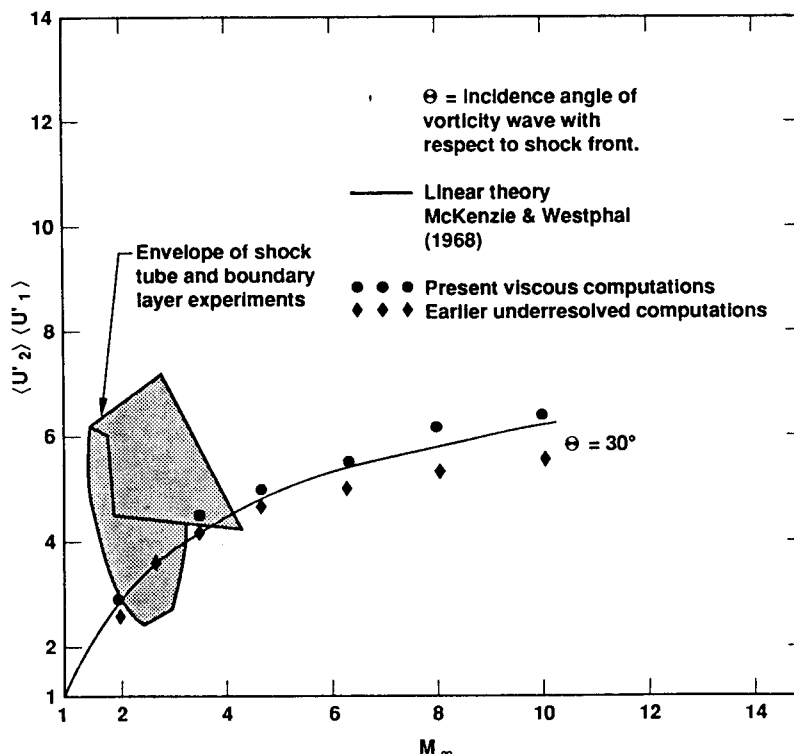


FIGURE 1. Amplification of turbulence intensity by Interactive passage of shock-wave numerical and experimental results.

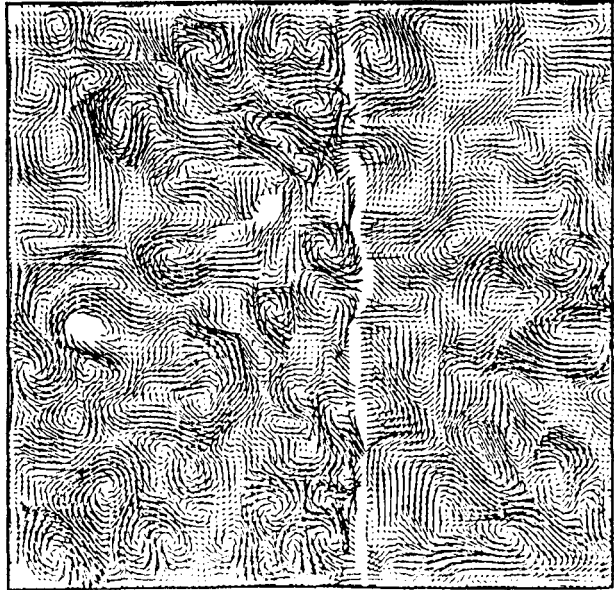


FIGURE 2. Variations to shock front and turbulent field caused by passage of Mach 2.3 shockwave (numerical results). Reprinted by permission, Ref. 4.

Figure 1 illustrates these pseudospectral transform method results using two forms of imbedded shock solutions. The more satisfactorily accurate results were developed at the expense of additional analytical and computer effort, using dynamic near shock-front mesh refinement and shock fitting. Linear theory (solid line) results are plotted for comparison. The ordinate shows the amplification of the streamwise component of turbulent intensity as a function of shockwave Mach Number. Also in Fig. 1, a cross-hatched envelope of experimental shockwave boundary layer, and reflected shockwave interaction (shock tube) results are shown.

Recently, high resolution Godunov procedure shockwave simulations have been applied to examine this interaction-amplification process [4]. Figure 2 shows a Mach 2.3 shock wave advancing through predeveloped turbulence. Note, particularly, that the computed shock front develops spatial distortions under the influence of the randomly inhomogeneous vorticity field into which it is moving.

## 2. SHOCK STRUCTURE

Almost 80 years ago, Taylor illustrated that, to leading order, the shock-front thickness depends directly on the statistically averaged molecular transport properties and inversely on the shock strength and density [5]. The present calculations are attempts to develop the mass, momentum and energy exchanges across a finite thickness shock-front region using eddy exchange scales rather than Taylor's molecular-scales for the integral flux conservation .

However, more accurate estimates of the energetic modal partition that develops between advancing shock and turbulent field

require consideration of higher-than-leading-order interactions. Strong coupling must be properly accounted for between all three competing modes (entropy, vorticity, acoustic). Kovasznay's [6] seminal analysis of almost 35 years ago indicates that strong coupling first emerges asymptotically at the third-order in modal coupling [6]. To pursue this, asymptotic analysis is applied here in combination with numerical results in interpretation of the energetics of the interactions. Examination of the developed attributes and implications of the asymptotic analysis requires more space than that allocated for this paper. Hence, its description will be reserved for a later publication.

## 2.1 Random Choice Shock-Front Description

A random selection Monte-Carlo procedure is used to develop the perturbation distribution functions normal to the advancing shock surface in association with a spectral collocation procedure, applied orthogonally, to simulate the tangential influence of the distortions along the shock. The simulated distortions are created by interactions with modeled upstream random disturbances. Following Taylor's original molecular concept [5] and the later Mott-Smith concept [8] for developing the shock-front velocity exchange relations by linearized combination of upstream, and downstream velocity distributions, we develop the requisite distribution functions parallel to shock-propagation direction. Our procedure is developed from ideas originated in Bird's [7] Monte-Carlo fluidynamic shock-wave computations.

Linearized integral combination of random valued fluxes of mass, momentum and energy, evaluated about preshock (subscript, 0) and postshock (subscript, 1) turbulent fields produce a streamwise ( $\xi$ ), integral finite shock thickness. Velocity and exchange scalar flux distributions are computed at a series of vertical locations ( $\eta$ ) along the turbulence-distorted shock front surface.

Each Monte-Carlo exchange distribution is considered a single, instantaneous realization for the streamwise  $\xi$  distribution profiles and consequent integral-length scales. Figures 3 and 4 show a superposition of realizations taken at randomly selected shock surface ( $\eta$ ) levels. The separately computed, distorted shock-front surface, is shown as a shock-front silhouette, on the right. Figures 3 and 4 are developed from results at shock Mach Numbers of 3 and 6, respectively. The distorted shock fronts are obtained separately from pseudospectral collocation calculations [3,10], or discrete Lagrange/Euler SHALE calculations [11]. The SHALE model for the preliminary "global" solutions is under current development. The qualitatively real contraction of the shock thickness with increasing Mach Number is also indicated in the figures although the

dimensions in the silhouettes are primarily established by the computational mesh, not physics!

The present Monte-Carlo procedure effectively magnifies the thickened shock-front region independently of, but indirectly based, on the gross silhouette features given by the global discrete mesh or collocation solutions. The shock-front, random-choice computations

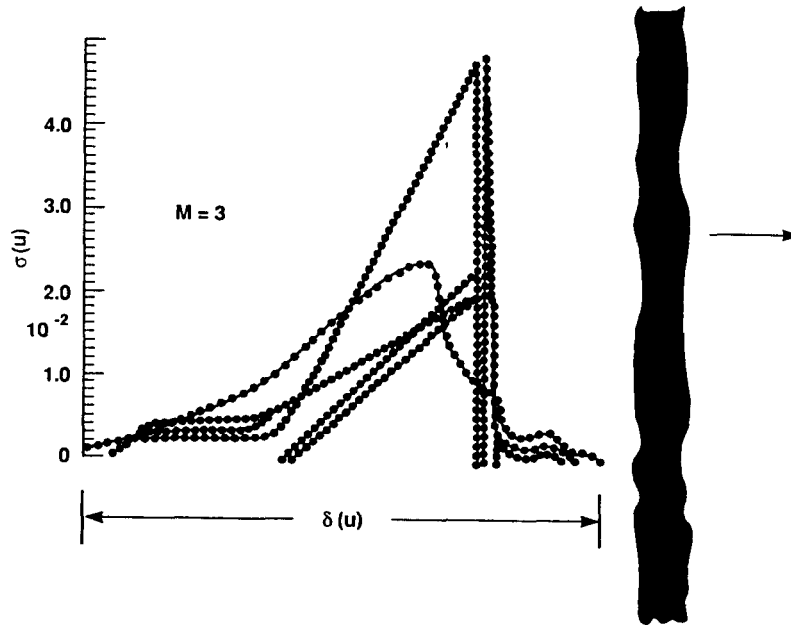


FIGURE 3. Velocity standard deviation for several realizations taken at various positions along the turbulence distorted shockfront shown as a silhouette ( $M_S=3.0$ ).

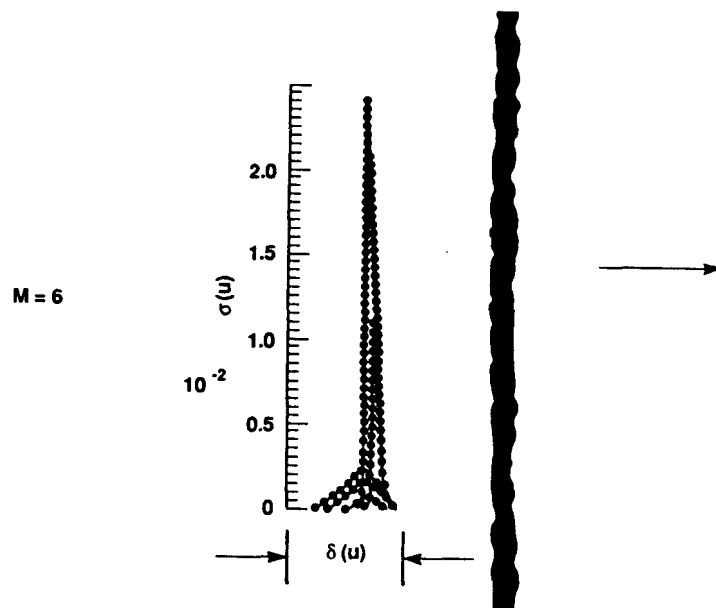


FIGURE 4. Velocity standard deviation for several realizations taken at various positions along the turbulence distorted shockfront shown as a silhouette ( $M_S=6.0$ ).

provide individual realizations for ensemble averaged physical shock thickness and velocity/flux distributions for the shock front in transit through prescribed levels of turbulence.

At this approximation level, we define the mean shockwave velocity,  $\vec{U}_N$ , with zero variance. Random flux exchange integrand contributions,  $\phi'_{(0)} - \phi'_{(1)}$  are defined for the streamwise shock transition realization computations, based on assumed (turbulent) randomness of both preshock and postshock material velocity components:

$$\vec{q}_{(i)} = \langle \vec{q}_{(i)} \rangle (\text{Mean}) + \vec{q}'_{(i)} (\text{Perturbational}), \quad (1)$$

where 
$$\vec{q}_{(i)}^2 = u_{(i)}^2 + v_{(i)}^2, \quad (2)$$

$$u_{(i)} = \frac{d\xi}{dt}, \quad v_{(i)} = \frac{d\eta}{dt},$$

and 
$$\phi'_{(i)} = (u'_{(i)} - \vec{U}_N). \quad (3)$$

To represent the collective random flux exchanges, the transition realization ( $\xi$  wise) integrands of mass, momentum and energy are identified by the symbol,  $\tilde{J}$ . In addition to the random velocities, we also identify transported passive scalars (II): density ( $\rho$ ), internal energy density ( $e$ ), and through an appropriate equation of state, the pressure ( $p$ ), viz.

$$p(\xi) = p(\rho, e). \quad (4)$$

In the test calculations, an ideal gas equation of state was used, with the polytropic exponents, 7/5 (conventional) or 5/3 (turbulent "model" gas) assigned.  $\tilde{J}$  is then associated with integrals of mass momentum and energy through a finite shock width,  $\Delta_s$ : Conditionally, conservation requires that,

$$\tilde{J} \equiv \left[ \begin{array}{l} dM(\xi) = \rho_0 \phi'_0 - \rho_1 \phi'_1 \quad (\text{Mass}) \\ dMu(\xi) = (\rho_0 u'_0) \phi'_0 - (\rho_1 u'_1) \phi'_1 + p'_0 - p'_1 \quad (\text{Momentum}) \\ dME(\xi) = \rho_0 q_0^2 \phi'_0 - \rho_1 q_1^2 \phi'_1 + 2(\rho_0 e_0 \phi'_0 - \rho_1 e_1 \phi'_1) \\ \quad + 2(\rho_0 u'_0 - \rho_1 u'_1) \quad (\text{Energy}) \end{array} \right] \quad (5)$$

(II) Passive Scalars refer to the level of approximation where significant density, energy, and pressure fluctuations are considered to develop only by passive (noninteractive) transport of the scalar quantities in a fluctuating velocity field.

$$\int_{\xi-\Delta_s/2}^{\xi+\Delta_s/2} \tilde{J} d\xi = 0, \quad (6)$$

over the integral domain,  $[\xi, \xi + \Delta_s]$ , where  $\Delta_s$  is to be determined.

To complete the system for integration, a global constraint on the tangential material velocity that is exact in a stationary system is applied in accord with central limit considerations for the random velocity field,

$$v_o = v_1, \text{ viz., one invokes} \\ \vec{q}_i = \langle q_i \rangle, i = 0, 1. \quad (7)$$

Equilibrium molecular thermodynamic consistency is assumed, permitting Eqn. (4) to represent the state globally. This is another statement of the conventional molecular-scale to eddy-scale separation and isolation.

Each of the distortions along the shock front contributes both streamwise and tangential (parallel to the vertical axis) perturbational components. The contributions of the ensemble of realizations over the entire surface is effectively combined by computing momentum, mass, and energy integrals over the two dimensions of a finite-thickness shock surface. The normal integrations include derivatives of both tangential and streamwise fluxes evaluated in phase space then transformed back to configuration space using an FFT collocation procedure.

These tangential derivatives are evaluated with respect to integral surface functions. The surface functions,  $\Lambda$ , must be continuous and analytic, at least through second derivatives,

$$\tilde{J} = \tilde{J}(\Lambda, \Lambda, \eta, \Lambda, \eta \xi, \Lambda, \eta \eta, \vec{q}, \rho, e), \quad (8)$$

to satisfy consistency and realizability of vorticity evolution at the continuously distorted shock surface. In a recent paper, Emanuel and Liu [9] provide compelling arguments for rigor in developing the critical tangential and normal derivatives at a continuous, two-dimensional curved shock surface or for an otherwise plane shock moving into a materially heterogeneous or an unsteady region. On reflection, all of these conditions are encountered in the physical situation under study here.

The results (which are, essentially, ensemble averages of the individual realizations over the entire shock surface) include

simulated probabilistic distributions of the velocity variance (essentially component contributions of the turbulent kinetic energy) and standard deviations of density and energy. The former distributions are shown on the left, while the density distributions are shown on the right in Fig. 5, for Mach Number 3.

## 2.2 Visco-elastic Response

The results of these calculations here are being used to develop information on the redistribution of energy between acoustic, entropy, and vortical fields excited by shock transition through turbulence. The global information sought is the partition of energy between directed shock translation and turbulence.

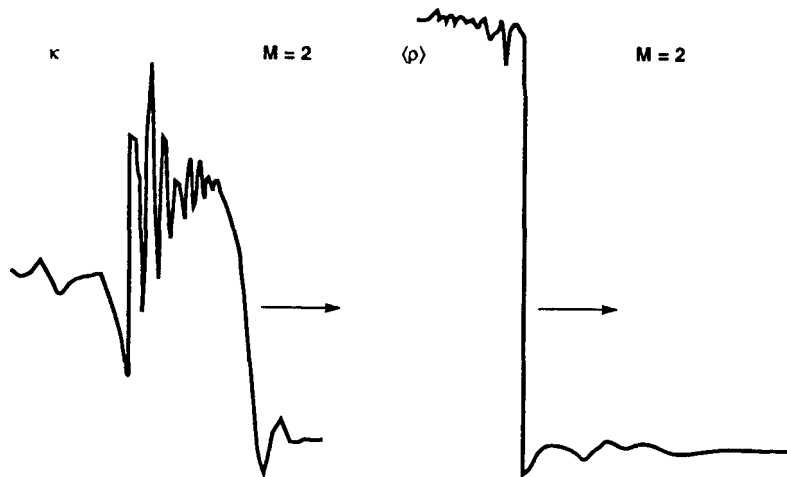


FIGURE 5. Turbulence kinetic energy profiles and density profiles in transition over a finite width shock front at Mach Number 2.

Emphasis also is placed on the modeling of the turbulent-field response to shock transition with a kinematic model, that could be efficiently implemented in existing computer codes for prediction of the shock-turbulent amplification process, and its temporal persistence after the shock front moves away.

Current attention has been placed on a linear visco-elastic response model for the shock-amplified turbulent domain. Its relationship to the dynamic response and relaxation of the turbulent field, as well as its relationship to artificial "viscous" damping term(s) used with shock-capturing schemes on discrete mesh simulations, are under current study [10].

Figure 6 illustrates the apparent redistribution of turbulence kinetic energy based on the present Monte Carlo averages, as well as a visco-elastic response model applied at the shock wave. In addition, we show a kappa-epsilon conventional turbulence single-

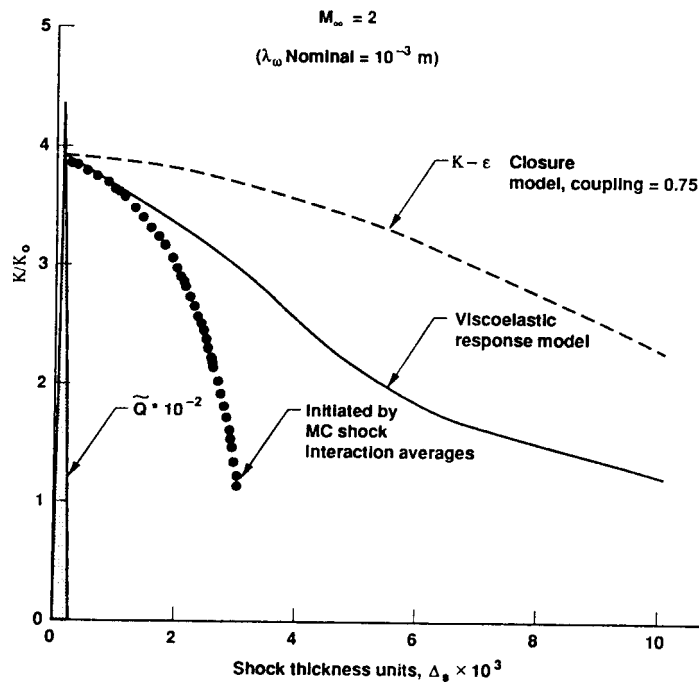


FIGURE 6. Comparison of turbulent kinetic energy profiles through shock transition as predicted by Monte Carlo results, visco-elastic response model results, a conventional kappa-epsilon model and artificial viscosity,  $Q$ , model. Mach No. = 2.0.

point closure model and also conventionally added shock oscillation damping artificial viscosity "Q". All results are remapped to a common shock thickness,  $\Delta_s$ , to assist comparison. The actual physical dimensions for the depicted results, of course, vary substantially depending on how the shock was resolved (fitting, tracking, or capturing) and the dimensions of the finite-mesh used.

### 3. CONCLUSIONS

- Random-choice integrals provide definition of shock thickening as well as time-and-space-scale dimensions for interaction of modal coupling components in shock-turbulence encounters.
- Information on direct-shock translational energy to turbulent kinetic energy may be developed from the results.
- Some support for a visco-elastic response model is developed from the random Monte-Carlo model results.
- The behavior of a conventional  $\kappa$ - $\epsilon$  model can be modified to approximate the shock-transition results by using different coupling coefficients between  $\kappa$ - $\epsilon$  evolution equations. However, care must be taken to insure consistency with the modeled persistence length of shock-generated turbulence behind the shock interaction region.

- The influence of Q added for shockwave damping in numerical calculations is offset and fully compensated for by the application of any reasonable turbulence eddy viscosity or turbulence shock response model.

#### 4. REFERENCES

1. Zang, T.A., M.Y. Hussaini, D.M. Bushnell, *AIAA J.* **22**, (1), 13-21, (1984).
2. McKenzie, J.F., K.O. Westphal, *PHYSICS OF FLUIDS*, **11**, (11), 2350-2362, (1968).
3. Buckingham, A.C., Proc. 5th International Conf., *Numerical Methods in Laminar and Turbulent Flow*, ed. C. Taylor, Pineridge Press, Swansea, UK, 963-974, (1987).
4. Rotman, D.A., P. Collela, Seminar, personal communications, Lawrence Livermore National Laboratory, Livermore CA, (1988).
5. Taylor, G.I., *Proc. Royal Society London, A*, **84**, 371-377, (1910).
6. Kovasznay, L.S.G., *J. AERO. SCI.*, **20**, (10), 657-682, (1953).
7. Bird, G.A., *J. FLUID MECH.*, **30**, 479-487, (1967).
8. Mott-Smith, H.M., *PHYS. REVIEW*, **82**, 885, (1951).
9. Emanuel, G., M.-S. Liu, *PHYSICS OF FLUIDS*, **31**, (12), 3625, (1988).
10. Buckingham, A.C., *41st Annual Mtg, Div. of Fluidynamics, American Physical Society*, State Univ. of New York, Buffalo NY, (1988).
11. Demuth, R.B., L.G. Margolin B.D. Nichols, T.F. Adams, B.W. Smith, *SHALE: A Computer Program for Solid Dynamics*, Los Alamos National Laboratory, LA-10236, Los Alamos NM (1985), and informal documentation, communications with L.G. Margolin on modifications to the fluiddynamic version SHALE code, Lawrence Livermore National Laboratory, Livermore CA, (1988-1989).